Magnetic instabilities of smectic-C liquid crystals

E. Meirovitch and Z. Luz
Department of Isotope Research, The Weizmann Institute of Science, Rehovot, Israel

S. Alexander
The Racah Institute of Physics, The Hebrew University, Jerusalem, Israel

(Received 3 June 1976)

We have investigated elastic deformations by external magnetic fields in flat samples of smectic C with fixed boundary conditions. In the calculations the internal parameters (tilt angle, density, interlayer distance) are assumed to be fixed, distortions of the smectic layers are neglected, and only reorientations of the director about the normal to the smectic layers are allowed. The problem is solved exactly assuming a one-dimensional variation of the order parameter. Stability conditions and explicit expressions for the orientation of the director as a function of position are derived for general orientations of the magnetic field. Solutions of the variational problem can be classified according to the maximum deviation angle, Φ, of the director. In general there are several separated allowed regions of Φ. When Fréedericksz transitions occur, they are usually discontinuous first-order transitions. The properties of the solutions are discussed and some special examples are considered in detail. Transitions are investigated both as a function of the magnitude and of the orientation of the magnetic field. Expressions for the free energy are also derived.

I. INTRODUCTION

The elastic theory of smectic C liquid-crystal phases[1,2] has been discussed by the Orsay group.[3] It was shown there that nine elastic constants are needed to describe the system when one assumes that the interlayer spacing and the tilt angle are constant. Rapini[4] has used this theory to discuss the behavior of single-crystal layers of smectic C in magnetic fields. He has shown that the analog of a Fréedericksz transition should be observable in this phase. Essentially these transitions involve the rotation of the director on the cone, determined by the normal to the smectic layers and the tilt angle.

The calculation of Rapini is patterned on the nematic case. It is, in fact, equivalent to the determination of a criterion for the stability of the initial state when a magnetic field is applied along suitable symmetry directions. We will show that this procedure is, in general, inadequate. A smectic C can have several locally stable configurations in a magnetic field. In such a situation the configuration resulting continuously from the initial state when the field is applied may remain locally stable (against small deformations) in spite of the fact that configurations of lower energy are available to the system. This gives rise to the usual difficulties in interpreting experimental results when first-order transitions are involved.

Instead of checking for the stability of an assumed state, we look explicitly for the solutions of the Euler-Lagrange equations resulting from the requirement that the sum of the magnetic and elastic energies should be extremal. The mathematical procedure in treating nematic slabs with oblique boundary conditions is analogous to that used by Onnagawa and Miyashita.[5]

We follow Rapini in restricting ourselves to flat smectic layers and boundary conditions determining the orientation of the director at the two boundaries of a parallel slab. Explicitly, we only discuss Rapini's type-N geometry (see Fig. 1) with layers parallel to the surface of the slab, but the general case only differs in that it involves different combinations of the elastic constants.

For simplicity, we assume that the magnetic-susceptibility tensor is axially symmetric with its unique axis defining the local orientation of the director $\vec{U}$. Experimentally this seems to be very nearly the case,[6] and the generalization of our results is straightforward. We discuss the solution

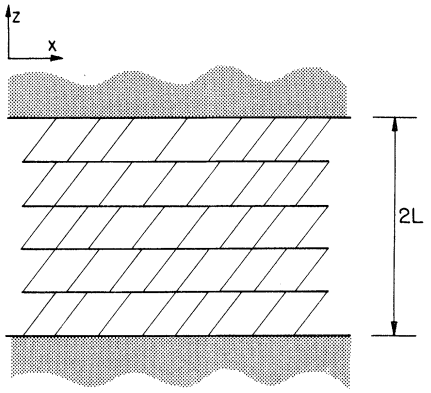

FIG. 1. Schematic diagram of a smectic C single-crystal layer.

as a function of the orientation of the magnetic field in the coordinate frame determined by the boundary conditions. For most orientations metastable states exist and first-order transitions have to be considered.

It should be noted that the extension of these results to a situation with curved layers is not immediate. It can be seen from the structure of the elastic energy[3] that the orientation of the director is coupled to the local curvature. When the layers are not flat, this gives rise to volume-anisotropy terms which complicate the calculation, and are neglected in our calculation.

II. THEORY

The geometry, coordinate system, and notation used in the calculations are described in Figs. 1 and 2. We consider a parallel slab of thickness $2L$ with boundaries and smectic layers parallel to the xy plane. The director $\vec{U}$ is tilted by the tilt angle ψ, and has an azimuthal angle $\phi(\vec{U}(\psi,\phi))$. As boundary conditions we assume $\phi(0)=\phi(2L)=0$, i.e., at the boundaries $\vec{U}_0$ is in the xy plane. The magnetic field has polar angles α, $\beta[H=H(\alpha,\beta)]$. The only variable is then the azimuthal angle ϕ, which is a function of the position in the slab $[\phi=\phi(z)]$. The elastic free-energy density becomes[4]

$$F_{el}=\tfrac{1}{2}B_3\left(\frac{d\phi}{dz}\right)^2 , \tag{2.1}$$

and the magnetic free-energy density is

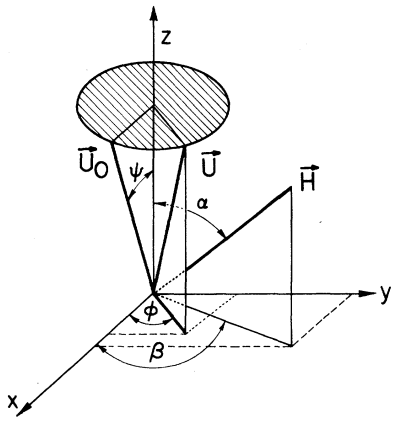

FIG. 2. Coordinate system for the smectic C phase: xy is the smectic plane. The director in the undistorted sample, $\vec{U}_0$, lies in the xz plane at an angle Ψ (the tilt angle) to z. $\phi(z)$ is the azimuthal angle of the (reoriented) director $\vec{U}$, and α,β are the polar and azimuthal angles of the magnetic field $\vec{H}$. The shaded area describes the base of the cone of the allowed orientations of the director.

$$F_{mag}=-\tfrac{1}{2}\chi_a(\vec{H}\cdot\vec{U})^2$$
$$=-\tfrac{1}{2}\chi_a H^2\sin^2\alpha\sin^2\psi$$
$$\times[\cos(\phi-\beta)+\cot\alpha\cot\psi]^2 , \tag{2.2}$$

where χ_a is the anisotropic part of the magnetic susceptibility (assumed to be positive);

$$\chi_a=\chi_{\parallel}-\chi_{\perp}>0 . \tag{2.3}$$

The total free energy per unit area of the slab (in units of $\frac{1}{2}\chi_a H^2\sin^2\alpha\sin^2\psi$) can then be expressed as

$$2\int_0^L dzF=2\int_0^L dz\{\xi^2\left(\frac{d\phi}{dz}\right)^2$$
$$-[\cos(\phi-\beta)+\cot\alpha\cot\psi]^2\} , \tag{2.4}$$

where F is the sum of the elastic and magnetic free-energy densities, and

$$\xi^2=B_3/(\sin^2\alpha\sin^2\psi\chi_a H^2) . \tag{2.5}$$

The Euler-Lagrange equation obtained by requiring that Eq. (2.4) be extremal, is

$$\xi^2\frac{d^2\phi}{dz^2}-[\cos(\phi-\beta)+\cot\alpha\cot\psi]\sin(\phi-\beta)=0 , \tag{2.6}$$

which has a first integral;

$$\xi^2\left(\frac{d\phi}{dz}\right)^2=[\cos(\Phi-\beta)+\cot\alpha\cot\psi]^2$$
$$-[\cos(\phi-\beta)+\cot\alpha\cot\psi]^2\equiv G(\Phi,\phi) . \tag{2.7}$$

The constant of integration was obtained by observing that $d\phi/dz=0$ when ϕ takes on its maximum value Φ. From symmetry, this maximum is at $z=L$, i.e., halfway between the plates.

From Eq. (2.7) we now obtain an expression for the second integral of the Euler equation;

$$\int_0^L\frac{dz}{\xi}=\frac{L}{\xi}\equiv h=\int_0^{\Phi}\frac{d\phi}{(G(\Phi,\phi)^{1/2}} , \tag{2.8}$$

where (from Eq. 2.5)

$$h=(HL\sin\alpha\sin\psi)(\chi_a/B_3)^{1/2} \tag{2.9}$$

is determined by the parameters of the problem. For given h the energy is thus extremal when the maximum tilt angle Φ is such that

$$h(\Phi)=\int_0^{\Phi}\frac{d\phi}{[G(\Phi,\phi)^{1/2}}=h . \tag{2.10}$$

Once we know the solution of Eq. (2.10) we can de-

termine z as a function of ϕ from

$$\frac{z(\phi)}{L}=\frac{1}{h}\int_0^{\phi}\frac{d\phi}{[G(\Phi,\phi)]^{1/2}}\ . \tag{2.11}$$

Since h is obviously real, one notes that ϕ is restricted to those ranges for which

$$G(\Phi,\phi)\geq 0;\quad 0\leq\phi/\Phi\leq 1\ . \tag{2.12}$$

These restrictions and their dependence on ψ, α and β are discussed in Sec. III.

For given ϕ we can substitute Eq. (2.8) into Eq. (2.4) to obtain an explicit expression for the *average* free energy per unit volume $\overline{F}$ of the slab,

$$\overline{F}=\int_0^L dzF(z)\Big/\int_0^L dz=\int_0^{\Phi}dF(\phi)\frac{dz}{d\phi}\Big/\int_0^{\Phi}d\phi\frac{dz}{d\phi}\ . \tag{2.13}$$

It is convenient to compute the energy as a function of Φ in the form

$$\overline{F}(\Phi)=\int_0^{\Phi}\frac{d\phi}{[G(\Phi,\phi)]^{1/2}}\{G(\Phi,\phi)-[\cos(\phi-\beta)+\cot\alpha\,\cot\psi]^2\}\Big/\int_0^{\Phi}\frac{d\phi}{[G(\Phi,\phi)]^{1/2}}\ . \tag{2.14}$$

This coincides with the true free energy when the extremum condition [Eq. (2.10)] holds. In practice, it is convenient to solve Eq. (2.10) graphically; we compute the integral $h(\Phi)$ as a function of Φ numerically. Solutions are then given by the points where $h(\Phi)$ has the specific value h. The free energy for these solutions is then proportional to $\overline{F}$, computed from Eq. (2.14). When several solutions exist for given h (i.e., H and L) it is possible to compare their energies. Some examples are discussed in Sec. IV.

Our derivation yields only a small number of stationary configurations for a given field, namely, those given by the implicit expression (2.11), where Φ satisfies Eq. (2.10). The lowest-energy configuration is always of this type. In general, however, these are *not* all the solutions of the Euler-Lagrange equation [Eq. (2.6)]; stationary configurations of higher energy do exist. There are two points where our derivation can be generalized:

(i) In choosing the integration constant in the first integral [Eq. (2.7)] we assumed that there is a maximum angle Φ for which $(d\phi/dz)_{\Phi}=0$. This excludes twisted configurations (analogous to cholesterics) which are of course possible but always have a higher elastic energy without any decrease in magnetic energy.

(ii) A similar generalization is possible in passing to the second integral [Eq. (2.8)]. In the form given we have assumed that $d\phi/dz$ has a unique sign, so that $\phi(z)$ is a monotonic function of z from $\phi=0$ to Φ [condition (2.12)]. Additional, nonmonotonic, solutions can be obtained if one allows more than one extremum $\{d\phi/dz=[G(\Phi,\phi)]^{1/2}=0\}$ where one can pass between two monotonic branches $\{d\phi/dz=[G(\Phi,\phi)]^{1/2}\}$ of the solution. Such solutions necessarily have nodes ($\phi=0, z\neq 0, 2L$). Thus, one has solutions of the type we have considered between any two nodes. The requirement that $d\phi/dz$ should be continuous at the nodes then implies:

$$\xi^2\left(\frac{d\phi}{dz}\right)^2_{\text{node}}=[\cos(\Phi_i-\beta)+\cot\alpha\,\cot\psi]^2=\text{const.}\ , \tag{2.15}$$

where the Φ_i are the extremal values of ϕ in the different intervals. This, together with the integral condition (2.8) for the interval between any two adjacent nodes, determines the solutions.

III. NATURE OF THE SOLUTIONS

Before presenting some results of numerical calculations for specific values of β and

$$a=-\cot\alpha\,\cot\psi\ , \tag{3.1}$$

we want to discuss the general features of the function $h(\Phi)$ defined in Eq. (2.10). As noted in (2.12), we require $G(\Phi,\phi)>0$ for ϕ varying continuously from zero to Φ, thus limiting the allowed ranges of Φ.

To determine these ranges and the limiting values of $h(\Phi)$ at the ends of the allowed regions, consider the function

$$P(\phi)=[\cos(\phi-\beta)-a]^2\ , \tag{3.2}$$

where

$$G(\Phi,\phi)=P(\Phi)-P(\phi)\ . \tag{3.3}$$

The condition (2.12), $0\leq\phi/\Phi\leq 1$, then implies

$$P(\Phi)\geq P(\phi)\ . \tag{3.4}$$

$P(\Phi)$ has extrema when

$$\frac{dP(\phi)}{d\phi}=-2[\cos(\phi-\beta)-a]\sin(\phi-\beta)=0\ . \tag{3.5}$$

For $|a|<1$ there are two minima $[\cos(\phi-\beta)-a=0]$ and two maxima $[\sin(\phi-\beta)=0]$. Examples of the function $P(\phi)$ for two special values of $|a|>1$, are shown in Fig. 3. When $|a|>1$, there is only one maximum and one minimum.

The allowed ranges of Φ follow immediately from Eq. (3.4), and the requirement that ϕ vary contin-

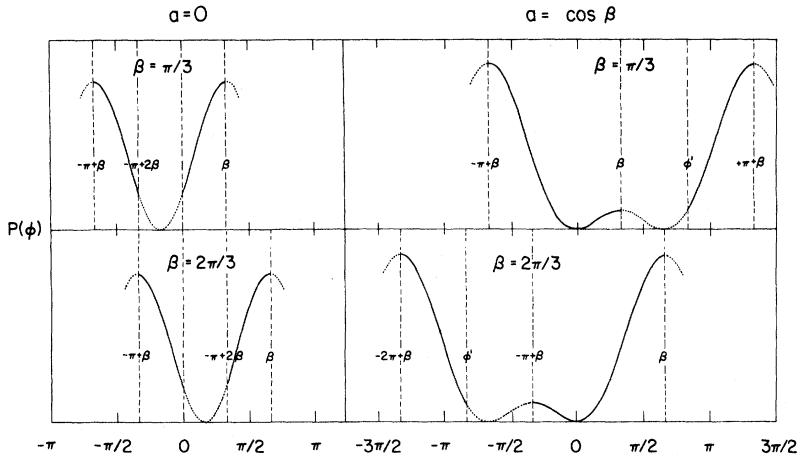

FIG. 3. Schematic plots of $P(\phi)$ [Eq. (3.2)] for two values of $a=-\cot\alpha\cot\Psi$. In each case plots are given for two values of the angle β. The allowed regions are drawn with heavy lines and are separated by dashed vertical lines.

uously from zero to Φ. They are listed in Table I, and for the cases shown in Fig. 3, are indicated by heavy lines. Clearly the problem is invariant under the transformation $\beta\to-\beta, \Phi\to-\Phi$. Also, since a reversal of the field ($\vec{H}\to-\vec{H}$) cannot change the torques, this transformation ($a\to-a$, $\beta\to\beta-\pi$) does not change any results. It is therefore sufficient to consider only the range $a\geq 0$, $0\leq\beta<\pi$.

We wish to investigate the behavior of $h(\Phi)$ [Eq. (2.10)] as Φ approaches the limits of the allowed ranges. The integrand in (2.10) diverges when $P(\phi)\to P(\Phi)$. This always happens when $\phi\to\Phi$, but can also happen at other points in the range of integration. There are three types of these potentially divergent contributions to the integral $h(\Phi)$ near the end points.

(i) Consider a region Δ near some point χ in the range of integration so that:

$$G(\Phi,\phi)=P(\Phi)-P(\phi)=A+P'(\chi)x\ ,$$
$$x=|\chi-\phi|\leq\Delta \text{ and } P'(\chi)\neq 0\ . \tag{3.6}$$

TABLE I. "Allowed" ranges of Φ [Eq. (3.4)]. $\Phi'=\arccos(2a-1)+\beta$; $\Phi''=-\arccos(2a-\cos\beta)+\beta$; $\gamma=\arccos(a)$; $0\leq\beta<\pi$.

	$0\leq a\leq 1$	
(a) $\beta<\gamma$	(A)	$(\beta-\pi)\longleftrightarrow\Phi''$
	(B)	$0\longleftrightarrow\beta$
	(C)	$\Phi'\longleftrightarrow\beta+\pi$
(b) $\beta>\gamma$	(A)	$\beta-\pi\longleftrightarrow 0$
$\lvert 2a-\cos\beta\rvert<1$	(B)	$\Phi''\longleftrightarrow\beta$
	(C)	$\Phi'\longleftrightarrow\beta+\pi$
(c) $\beta>\gamma$	(A)	$\beta-\pi\longleftrightarrow 0$
$\lvert 2a-\cos\beta\rvert>1$	(B)	$2\beta\longleftrightarrow\beta+\pi$
	$a\geq 1$	
(d)	(A)	$\beta-\pi\longleftrightarrow 0$
	(B)	$2\beta\longleftrightarrow\beta+\pi$

At the end point, $A\to 0$. The relevant contribution to $h(\Phi)$ is:

$$\int_0^\Delta \frac{dx}{[A+P'(\chi)x]^{1/2}}=\frac{2}{[P'(\chi)]^{1/2}}\times\left[\left(\Delta+\frac{A}{P'(\chi)}\right)^{1/2}-\left(\frac{A}{P'(\chi)}\right)^{1/2}\right], \tag{3.7}$$

which is finite as $A\to 0$. It follows that $h(\phi)$ remains finite. Any general point within the allowed range is of this type. Also the two points $\chi=0$ and Φ, $|\phi|>\phi'=|-\pi+2\beta|$, for $a=0$ (see Fig. 3) belong to this class.

(ii) $P'(\chi)=0$, so that

$$G(\Phi,\phi)=A+\tfrac{1}{2}|P''(\chi)|x^2\ , \tag{3.8}$$

and again $A\to 0$ at the end point. We have

$$\int_0^\Delta \frac{dx}{(A+\frac{1}{2}|P''(\chi)|x^2)^{1/2}}=\left(\frac{2}{|P''(\chi)|}\right)^{1/2}\times\ln\left[\Delta\left(\frac{|P''(\chi)|}{2A}\right)^{1/2}+\left(\Delta^2\frac{|P''(\chi)|}{2A}+1\right)^{1/2}\right], \tag{3.9}$$

so that the integral diverges logarithmically (as $\ln A$) as Φ approaches the end point. The contribution from the maximum at β near the end point Φ' for $a=\cos\beta$, $\beta=\frac{1}{3}\pi$ in Fig. 3 is of this type.

(iii) $P(\Phi)$ has a maximum at χ, e.g., $\chi=\beta$, for $a=0$ in Fig. 3. We want $h(\Phi)$ as $\Phi\to\chi$:

$$G(\Phi,\phi)=-\tfrac{1}{2}|P''(\chi)|(X^2-x^2)\ ,$$
$$X=\chi-\Phi;\quad x=\chi-\phi;\quad X<x<\Delta\ , \tag{3.10}$$

so that the contribution to $h(\Phi)$ is

$$\left(\frac{2}{|P''(\chi)|}\right)^{1/2}\int_X^{\Delta}\frac{dx}{(x^2-X^2)^{1/2}}=\left(\frac{2}{|P''(\chi)|}\right)^{1/2}\times\ln\left[\frac{\Delta}{X}+\left(\frac{\Delta^2}{X^2}-1\right)^{1/2}\right], \quad (3.11)$$

which again gives a logarithmic divergence as $\Phi\to\chi$.

Finally, there is one special case. When $a=-1$ and $\beta=0$,

$$P(\Phi)=(\cos\Phi-1)^2\approx\tfrac{1}{4}\Phi^4 \quad (3.12)$$

for small Φ. Thus

$$h(\Phi)=2\int_0^{\Phi}\frac{d\phi}{(\Phi^4-\Phi^4)^{1/2}}, \quad (3.13)$$

and one sees that

$$2/|\Phi|<h(\Phi)<4/|\Phi|, \quad (3.14)$$

so that there is a very strong $1/|\Phi|$ divergence as $\Phi\to 0$. It should be noted that $\Phi=0$ is not really an end point. However, for $\beta=0$ as $a\to-1$, two end points converge towards $\Phi=0$. The $|\Phi|^{-1}$ divergence is the limiting behavior of the logarithmic divergence (for $a>-1$) in this limit.

IV. RESULTS AND DISCUSSION

In the following we analyze and discuss in some detail a number of geometries. We first consider a geometry in which the magnetic field is in a plane perpendicular to $\vec{U}_0$, the direction of the undistorted director. We then discuss three other geometries, one in which the magnetic field lies in the smectic (xy) plane, and two cases in which it lies in a meridian plane with a constant azimuthal angle $\beta=0$ and 130°, and varying values of the polar angle α.

For each plane the integrals Eqs. (2.8) and (2.14) were computed for selected orientations of the magnetic field by numerical integration in the regions of allowed Φ values. The results of the computations are presented as plots of h and of $\bar{F}$ vs Φ. Based on these plots we then discuss the possible distortions in the director's alignment and phase transitions.

A. Magnetic field in a plane perpendicular to $\vec{U}_0$

For this configuration we have $\vec{H}\cdot\vec{U}_0=0$, i.e.,

$$a=-\cot\alpha\cot\psi=\cos\beta, \quad (4.1)$$

and thus a is fixed by the value of β. Plots of h and $\bar{F}$ for selected values of β between 0 and π are shown in Fig. 4. Note that plots for $\pi-\beta$ are obtained from those of β by the transformation $\Phi\to-\Phi$ as expected for this geometry. It is clear that $\Phi=0$ is always a solution (Φ_0) in this geometry, for any field, however, above a certain field one obtains additional solutions.

As an example, consider the case $\beta=30°$ in Fig. 4. In addition to Φ_0 there are two concave branches of solutions in the $h(\Phi)$ plots. The one for large positive Φ corresponds to much higher energies and is therefore not interesting. In the other branch we have defined three "critical fields," h_1, h_2, and h_3. To understand the meaning of these different solutions we consider the energy as a continuous function of the maximum angle Φ which is taken as an order parameter. Implicitly this implies that Φ is somehow determined externally and the Euler-Lagrange equation is, in general, not obeyed at $z(\Phi)$. The solutions we have derived are the stationary points of these $\bar{F}(\Phi)$ energy profiles and can be minima, maxima, or inflection points. In Fig. 5 are shown schematic diagrams

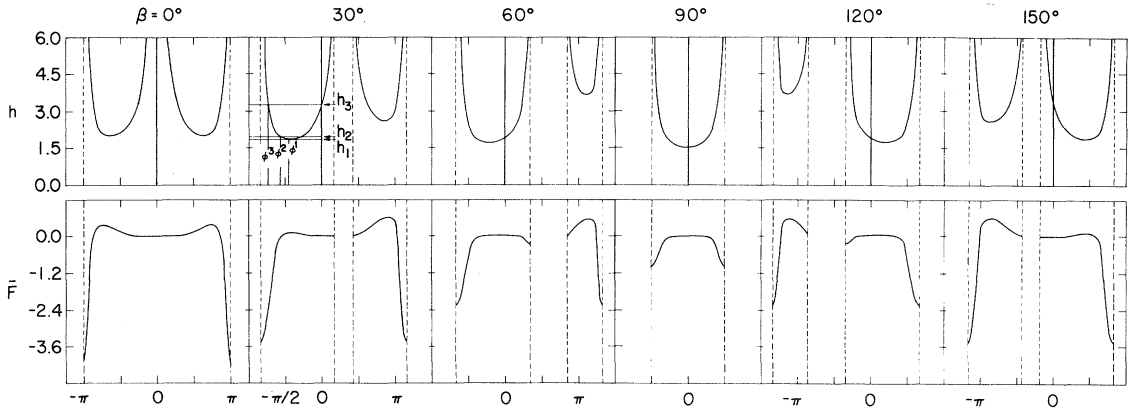

FIG. 4. h- [Eq. (2.8)] and $\bar{F}$- [Eq. (2.14)] vs-Φ plots for $a=-\cot\alpha\cot\Psi=\cos\beta$ and various β values. In the plot for $\beta=30°$ are indicated the critical fields h_1, h_2, and h_3 and the corresponding angles Φ^1, Φ^2, and Φ^3, discussed in the text. The vertical dashed lines separate allowed and forbidden regions of Φ. Note that the scale for $\bar{F}$ is in units of $\frac{1}{2}\chi_a H^2\sin^2\alpha\sin^2\Psi$.

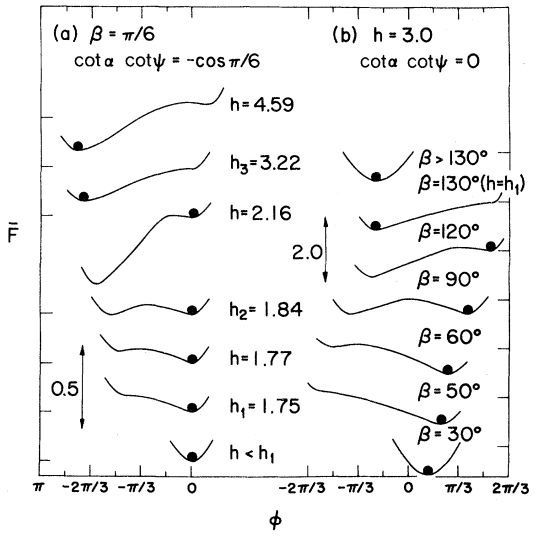

FIG. 5. Schematic diagrams of the average free-energy density as function of the maximum deflection of the director Φ at $z = L$. (a) The magnetic field is perpendicular to $\vec{U}_0$, at $\beta = 30°$ and the various diagrams correspond to increasing values of h. (b) The magnetic field is in the smectic plane with $h = 3.0$, and the various diagrams correspond to different values of β. The $\bar{F}$ values at the extrema are solutions of the Euler-Lagrange equation and were taken from Figs. 4 and 7, respectively, while the lines connecting the extrema are qualitative. The motion of the "ball" represents phase transitions that "must occur".

of $\bar{F}$ profiles for $\beta = 30°$ and various h values. The extrema in the plots are taken from Fig. 4, while the smooth curves connecting them are qualitative, and represent the expected trend in $\bar{F}$ as Φ deviates from these extrema. Clearly in all cases, for large $|\Phi|$'s the energy becomes large and positive.

Thus at low fields where Φ_0 is the only solution, this solution must be a minimum. As the field is increased a point is reached, h_1, at which one other solution ($\Phi^1 \sim -75°$) is obtained. Since the energy at Φ_0 is lower than that for Φ^1, Φ_0 must correspond to the stable configuration and the second solution must correspond to an inflection point in the free-energy profile (see Fig. 5).

Above h_1 there are, in general, three solutions for Φ (excluding the second high-energy branch) and from the plots of $\bar{F}$ it follows that as long as $h < h_3 \Phi_0$ corresponds to a local minimum. The other two solutions correspond respectively to a local maximum (Φ_{max}) and a local minimum (Φ_{min}). As h increases the energy corresponding to Φ_{min} decreases until at $h = h_2$ the free energies of both minima become equal. We define the value of Φ_{min} at this point as Φ^2. Above this value of the field the energy corresponding to Φ_{min} is lower than that for Φ_0 and a first-order phase transition can occur. However, the transition may be hindered by the barrier corresponding to Φ_{max} and therefore will not necessarily take place. As the field is increased further a point is reached, h_3, at which $\Phi_{max} = \Phi_0 = 0$. This point corresponds to an inflection point; the configuration becomes unstable and a first-order transition must result by an abrupt slip of Φ from Φ_0 to Φ_{min}. We define Φ_{min} at this value of h as Φ^3. As the field is increased above h_3 there are again three solutions for this branch, but now Φ_0 is a maximum in the free-energy profile and the local minimum at negative Φ's remains the more stable configuration.

There are two special directions for the magnetic field in this plane. When $\beta = 0$ the two branches of solution are symmetrically located with respect to Φ_0 as expected, since positive and negative distortions are equivalent. The field h_1 corresponds to $\Phi^1 = \pm 114°$ and h_2 to $\Phi^2 = \pm 148°$. However, the critical field h_3 is infinite and a phase transition does not necessarily occur. This configuration was studied by Rapini for a nonaxial magnetic susceptibility. Since we have assumed uniaxiality, the second-order phase transition found by him is not obtained in the present treatment.

The second special geometry, also studied by Rapini, corresponds to $\beta = \frac{1}{2}\pi$. Here $h_1 = h_2 = h_3 = \frac{1}{2}\pi$, and the phase transition is clearly second order, with a critical field

$$H_c = \frac{\pi}{2L \sin\psi} \left(\frac{B_3}{\chi_a}\right)^{1/2} . \tag{4.2}$$

To sum up the results for the orientation in which the magnetic field is in a plane perpendicular to $\vec{U}_0$, we plot in Fig. 6 the critical fields h_1, h_2, and h_3, as well as the corresponding values for Φ^i (in units of $\beta - \pi$) versus the angle β. It is seen that for field orientations not too close to the y direction there is an abrupt first-order change in the director bringing Φ close to $(-\pi + \beta)$, i.e., to the direction that minimizes the magnetic energy. However, when the magnetic field lies near the y axis ($\beta \sim 90°$), the transition is second order (or very nearly so) and the director will change smoothly from the undistorted configuration as the magnetic field is increased above the critical field.

It is instructive to discuss these results in terms of an expansion of the free energy in the "order parameter" Φ as in Landau's theory. For small ϕ we can expand the free-energy density

$$\begin{aligned} F(z) &= \xi^2 \left(\frac{d\phi}{dz}\right)^2 - [\cos(\phi - \beta) - \cos\beta]^2 \\ &\approx \xi^2 \left(\frac{d\phi}{dz}\right)^2 - \sin^2\beta\, \phi^2 + \sin\beta \cos\beta\, \phi^3 \\ &\quad - (\tfrac{1}{4} - \tfrac{7}{12}\sin^2\beta)\phi^4 + \cdots . \end{aligned} \tag{4.3}$$

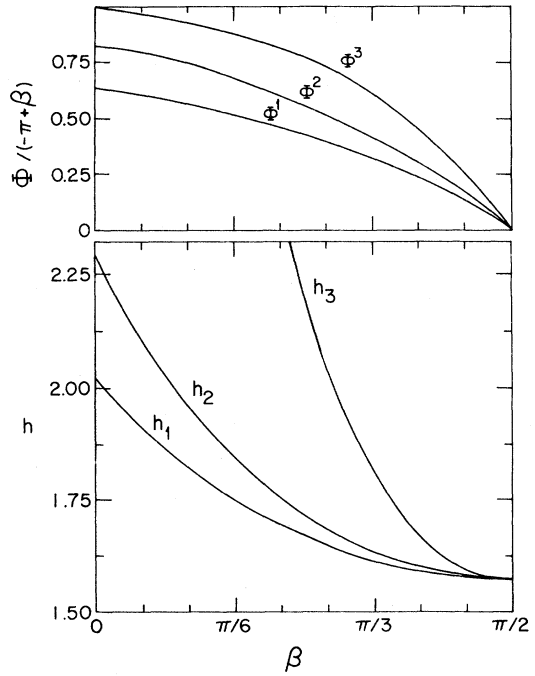

FIG. 6. Plots of the critical fields h_1, h_2, h_3 and the corresponding angles Φ^1, Φ^2, Φ^3 [in units of $(-\pi+\beta)$] vs the azimuthal angle β for a geometry in which the magnetic field lies in a plane perpendicular to $\vec{U}_0$.

To satisfy the boundary conditions we can expand;

$$\phi(z)=\sum_k \Phi_k \sin\frac{\pi kz}{2L} . \tag{4.4}$$

It is clear from the form (4.3) that an instability of the most unstable mode $k=1$ is necessary if one wants to get solutions other than $\phi=0$. Retaining only this mode one has

$$\overline{F}=\int_0^L \frac{F(z)dz}{L} \simeq \left(\xi^2\frac{\pi^2}{8L^2}-\tfrac{1}{2}\sin^2\beta\right)(\Phi_1)^2 + \frac{4}{3\pi}\sin\beta\cos\beta(\Phi_1)^3 - \tfrac{3}{32}(1-\tfrac{7}{3}\sin^2\beta)(\Phi_1)^4+\cdots . \tag{4.5}$$

We can thus determine h_3 from the coefficient of $(\Phi_1)^2$;

$$h_3=\pi/(2\sin\beta) , \tag{4.6}$$

since the expansion certainly gives the local stability of Φ_0 exactly. The presence of a finite term in $(\Phi^1)^3$ assures that the transition is generally first order.

For the special case $\beta=\frac{1}{2}\pi$ the coefficient of $(\Phi^1)^3$ vanishes and the transition is continuous with critical field at

$$h=\tfrac{1}{2}\pi(=h_3) , \tag{4.7}$$

as in Eq. (4.2).

When $\beta=0$ the cubic term also vanishes. In this case the coefficient of $(\Phi^1)^2$ remains positive for all fields ($h_3\to\infty$). The quartic term is, however, negative and, as is seen in Fig. 4, the transition is first order.

B. Magnetic field in the smectic plane

For this plane $\alpha=\frac{1}{2}\pi$ and

$$a=-\cot\alpha\cot\psi=0 \tag{4.8}$$

for all orientations of the magnetic field. Some representative plots of h and $\overline{F}$ vs Φ are shown in Fig. 7. It is sufficient to consider the range $0\le\beta\le\frac{1}{2}\pi$ because, for $a=0$:

$$P(\Phi,\beta)=P(\Phi,\pi+\beta)=P(-\Phi,\pi-\beta) . \tag{4.9}$$

For general β, $h(\Phi)$ has two branches, a monotonic branch increasing from zero for $\Phi=0$, which diverges at β, and, in the range $-\pi+2\beta>\Phi>-\pi+\beta$ a concave branch which is finite at the upper end and diverges at the lower end of the range (see Fig. 3). Thus, for a finite magnetic field $\Phi=0$ is not a solution of the Euler-Lagrange equation and there is a continuous distortion of the director along the first branch as the magnetic field increases from zero. Two special orientations are $\beta=0$ for which $\Phi=0$ is a solution and is, in fact, the only minimum of the free energy for all finite

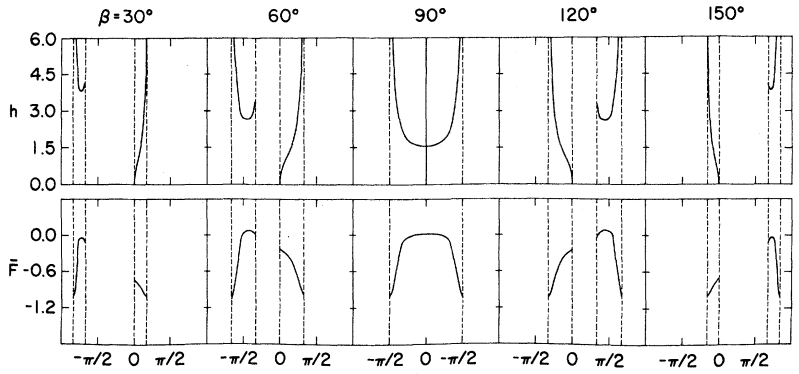

FIG. 7. Same as in Fig. 4 for the magnetic field in the smectic plane ($\cot\alpha\cot\Psi=0$).

values of H, and $\beta = \frac{1}{2}\pi$, which is identical to the case $\beta = \frac{1}{2}\pi$ for $a = \cos\beta$ discussed above (Fig. 4).

As before we define the critical field h_1 as the lowest field for which two solutions for Φ are obtained. This corresponds to an inflection point in the free-energy profile [see Fig. 5(b)]. Just above h_1 there are three solutions for Φ. A minimum at $0 < \Phi < \beta$, another local minimum but of higher energy at $\Phi \lesssim -\pi + \beta$, separated by a maximum at $\Phi \gtrsim -\pi + 2\beta$. As h increases the free energies at the two minima approach each other but do not cross. Consequently no abrupt jumps in Φ will occur at finite fields (except for $\beta = \frac{1}{2}\pi$ when there is a second-order transition).

One notes that the "third" solution describing the maximum which moves to $-\pi + 2\beta$ as the field is increased, disappears above some h value. Physically there must be a metastable maximum which separates states which decay into the two minima. Thus a third solution of the Euler-Lagrange equations must exist for all fields with a Φ between the two minima. In fact it can be shown that the original maxima deform continuously into symmetric solutions with two nodes ($\Phi = 0$), i.e., belonging to the second generalization b described in Sec. II. These solutions are not drawn in Fig. 7, but for the simple case $a = 0$ they can readily be derived from those already drawn:

$$\bar{h}(\Phi) = h(\Phi) + 2h(-\pi + 2\beta - \Phi), \quad -\pi + \beta < \Phi < -\pi + 2\beta \ . \tag{4.10}$$

An abrupt jump in Φ may, however, be effected by the following experiment. The magnetic field is oriented in the smectic plane at some angle $0 < \beta < \frac{1}{2}\pi$ and its strength increased to above the critical field H_c [Eq. (4.2)]. The director will then lie along the positive branch with $0 < \Phi < \beta$. When the magnetic field is rotated in the smectic plane to $\beta = \frac{1}{2}\pi$, Φ will remain on the positive side of the solution, but as β is increased beyond $\frac{1}{2}\pi$ the positive solution of Φ becomes metastable since it now corresponds to the local minimum in the concave branch of higher energy than that for the negative Φ solution and an abrupt jump to the negative branch may occur. However, this process requires activation energy since the two minima are separated by an energy barrier. If the flipping over of the director does not occur, it may still be affected by increasing β to the orientation for which h corresponds to the critical field h_1. At this geometry the positive solution for Φ corresponds to an inflection point in the free-energy profile and a flip over to negative Φ must occur abruptly. The changes in the free-energy profile on rotation of the magnetic field in the smectic plane are schematically illustrated in Fig. 5(b).

C. Magnetic field in meridian planes

In this section we consider geometries in which the magnetic field is confined to planes with a constant azimuthal angle β. A particularly interesting case is the plane with $\beta = 0$, i.e., the xz plane. For this case with $0 > \alpha > \frac{1}{2}\pi$ ($\cot\alpha \cot\psi > 0$) there is only one solution for the Euler-Lagrange equation, i.e., $\Phi = 0$ for all z, and therefore no reorientation of the director on application of a magnetic field is expected. However for $\alpha > \frac{1}{2}\pi$ (negative $\cot\alpha \cot\psi$) more solutions are possible, and depending on the magnitude of $\cot\alpha \cot\psi$ the system might undergo a first-order phase transition. In Fig. 8 are shown h- and $\bar{F}$-vs-Φ plots for three negative values of the parameter $\cot\alpha \cot\psi$. Clearly for all orientations in this plane $\Phi = 0$ is a solution and the additional branches of solutions are symmetric about zero as expected from the symmetry of the problem. The plot for $\cot\alpha \cot\psi = -0.75$ is typical for orientations for which this parameter is between zero and -1. The two limiting values 0 and -1 are special orientations of cases A and B, and were discussed before. As in the discussion above we may define a critical field h_1 corresponding to the appearance of inflection points, and h_2 which the energies of the minima at $\Phi \neq 0$ equal the energy at $\Phi = 0$. For h values larger than h_2 the minima at $\Phi \neq 0$ are lower than the local minima at $\Phi = 0$. However, there is no finite field corresponding to h_3 at which the energy surface at $\Phi = 0$ becomes an inflection point or a maximum so as to force the system to undergo a phase transition.

When $\cot\alpha \cot\psi < -1$ the situation is quite different, as may be seen from the example corresponding to $\cot\alpha \cot\psi = -1.25$. It is easy to see, using a similar analysis as that described in connection with Fig. 4, that in addition to h_1 and h_2 there is a

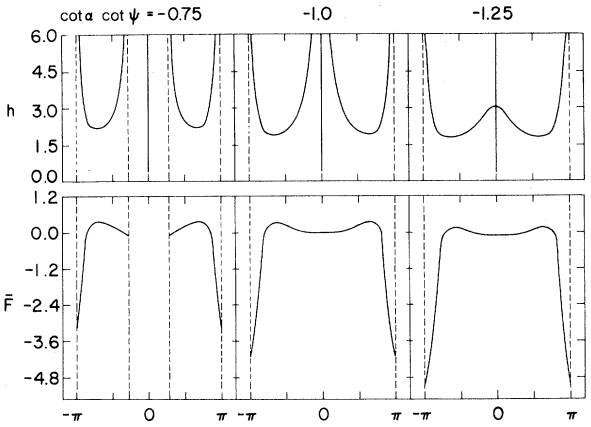

FIG. 8. Same as in Fig. 4 for the magnetic field in the meridian plane with $\beta = 0°$ and varying values of $\cot\alpha \cot\Psi$.

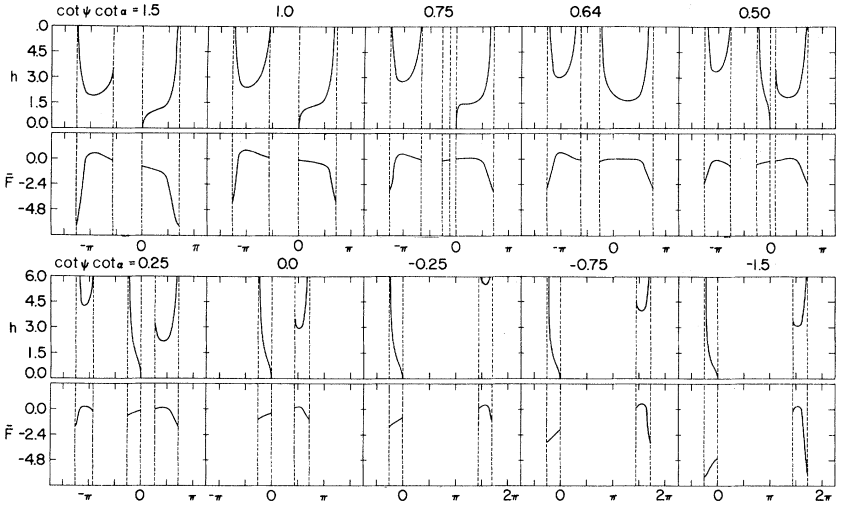

FIG. 9. Same as in Fig. 4 for a meridian plane with $\beta = 130°$.

finite field h_3 for which the energy at $\Phi = 0$ becomes a maximum. Consequently in magnetic fields corresponding to h_3 a first-order transition must occur by either a right- or a left-hand twist of the director around the z direction.

For geometries in which the magnetic field is oriented in a general meridian plane ($\beta \neq 0$) the situation is more complicated. Examples of h- and $\bar{F}$-vs-Φ plots for $\beta = 130°$ and varying $\cot\alpha \cot\psi$ are shown in Fig. 9. For a fixed tilt angle ψ these plots correspond to change in the polar angle α from close to the z direction to $-z$. Although the analysis of these plots is more involved than those of the previous planes, the general picture is quite similar. In particular it may be seen that it is possible to effect an abrupt flip of the director by rotating the magnetic field from, e.g., a large positive value of $\cot\alpha \cot\psi$ down to sufficiently low values of this parameter. In this case the magnetic field strength is adjusted so that $h > h_1$, where h_1 is the (first) critical field in the geometry corresponding to $\cot\alpha \cot\psi = -\cos\beta$ (+ 0.64 in Fig. 9). It may be shown by similar arguments to those presented above for case B, that when the direction of the magnetic field (i.e., α) is changed through this value of $\cot\alpha \cot\psi$, a geometry may be reached for which h will correspond to h_1. At this point the orientation of the director becomes unstable and a flip over must occur.

As yet no direct measurements on layered single-domain structures of smectic C were made to check this theory. Some measurements, however, were made on bulk multidomain samples.[7] It was found that the distortions caused by high magnetic fields were irreversible, i.e., after decreasing H, the original orientation of the director was not recovered, contrary to the prediction of the present theory. It seems that in these bulk samples, other factors, such as the curvature of the smectic plane, must be taken into account in order to explain the experimental observations.

ACKNOWLEDGMENT

This work was supported in part by the United States–Israel Binational Science Foundation.

[1]P. G. de Gennes, *The Physics of Liquid Crystals* (Clarendon, Oxford, 1974).
[2]M. J. Stephen and J. P. Straley, Rev. Mod. Phys. 46, 617 (1974).
[3]Orsay Group on Liquid Crystals, Solid State Commun. 9, 653 (1971).
[4]A. Rapini, J. Phys. (Paris) 33, 237 (1972).
[5]H. Onnagawa and K. Miyashita, Jpn. J. App. Phys. 13, 1741 (1974).
[6]Z. Luz and S. Meiboom, J. Chem. Phys. 59, 275 (1973); Z. Luz, R. C. Hewitt, and S. Meiboom, J. Chem. Phys. 61, 1758 (1974).
[7]E. Meirovitch and Z. Luz, Mol. Phys. 30, 1589 (1975).